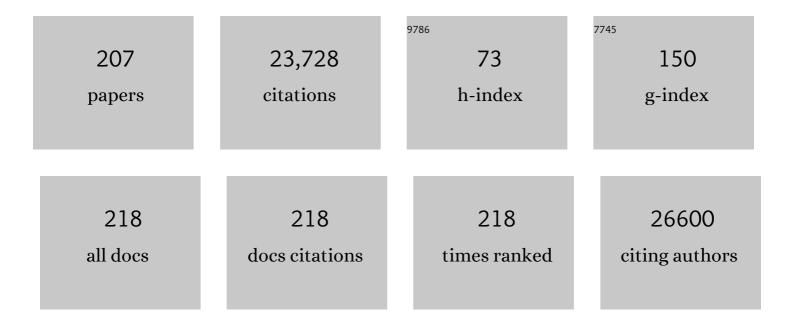
List of Publications by Year in descending order

Source: https://exaly.com/author-pdf/8433532/publications.pdf

Version: 2024-02-01



#	Article	IF	CITATIONS
1	Advances in methods and algorithms in a modern quantum chemistry program package. Physical Chemistry Chemical Physics, 2006, 8, 3172-3191.	2.8	2,597
2	Advances in molecular quantum chemistry contained in the Q-Chem 4 program package. Molecular Physics, 2015, 113, 184-215.	1.7	2,561
3	Nitrogen Fixation by Ru Single-Atom Electrocatalytic Reduction. CheM, 2019, 5, 204-214.	11.7	739
4	On the mechanism of enhanced oxygen reduction reaction in nitrogen-doped graphene nanoribbons. Physical Chemistry Chemical Physics, 2011, 13, 17505.	2.8	646
5	On the Theory of Organic Catalysis "on Water― Journal of the American Chemical Society, 2007, 129, 5492-5502.	13.7	587
6	Suppression of Hydrogen Evolution Reaction in Electrochemical N ₂ Reduction Using Single-Atom Catalysts: A Computational Guideline. ACS Catalysis, 2018, 8, 7517-7525.	11.2	545
7	Strengthening effect of single-atomic-layer graphene in metal–graphene nanolayered composites. Nature Communications, 2013, 4, 2114.	12.8	520
8	Software for the frontiers of quantum chemistry: An overview of developments in the Q-Chem 5 package. Journal of Chemical Physics, 2021, 155, 084801.	3.0	518
9	Scaled opposite-spin second order MÃ,ller–Plesset correlation energy: An economical electronic structure method. Journal of Chemical Physics, 2004, 121, 9793-9802.	3.0	492
10	Unprecedented high-temperature CO2 selectivity in N2-phobic nanoporous covalent organic polymers. Nature Communications, 2013, 4, 1357.	12.8	456
11	Active Sites of Au and Ag Nanoparticle Catalysts for CO ₂ Electroreduction to CO. ACS Catalysis, 2015, 5, 5089-5096.	11.2	434
12	Single-atom catalysts for CO ₂ electroreduction with significant activity and selectivity improvements. Chemical Science, 2017, 8, 1090-1096.	7.4	430
13	The High Performance of Crystal Water Containing Manganese Birnessite Cathodes for Magnesium Batteries. Nano Letters, 2015, 15, 4071-4079.	9.1	400
14	Electrochemical and Thermal Properties of NASICON Structured Na ₃ V ₂ (PO ₄) ₃ as a Sodium Rechargeable Battery Cathode: A Combined Experimental and Theoretical Study. Journal of the Electrochemical Society, 2012, 159, A1393-A1397.	2.9	316
15	Na ₂ FeP ₂ O ₇ as a Promising Ironâ€Based Pyrophosphate Cathode for Sodium Rechargeable Batteries: A Combined Experimental and Theoretical Study. Advanced Functional Materials, 2013, 23, 1147-1155.	14.9	316
16	Entropy and the driving force for the filling of carbon nanotubes with water. Proceedings of the National Academy of Sciences of the United States of America, 2011, 108, 11794-11798.	7.1	287
17	Intermolecular π-to-π Bonding between Stacked Aromatic Dyads. Experimental and Theoretical Binding Energies and Near-IR Optical Transitions for Phenalenyl Radical/Radical versus Radical/Cation Dimerizations. Journal of the American Chemical Society, 2004, 126, 13850-13858.	13.7	286
18	Two-Dimensional Transition Metal Dichalcogenide Monolayers as Promising Sodium Ion Battery Anodes. Journal of Physical Chemistry C, 2015, 119, 26374-26380.	3.1	279

#	Article	IF	CITATIONS
19	Electrochemical ammonia synthesis: Mechanistic understanding and catalyst design. CheM, 2021, 7, 1708-1754.	11.7	253
20	Balancing activity, stability and conductivity of nanoporous core-shell iridium/iridium oxide oxygen evolution catalysts. Nature Communications, 2017, 8, 1449.	12.8	250
21	Hydrated Intercalation for Highâ€Performance Aqueous Zinc Ion Batteries. Advanced Energy Materials, 2019, 9, 1900083.	19.5	243
22	Ab Initio Study of the Sodium Intercalation and Intermediate Phases in Na _{0.44} MnO ₂ for Sodium-Ion Battery. Chemistry of Materials, 2012, 24, 1205-1211.	6.7	223
23	Activated TiO2 with tuned vacancy for efficient electrochemical nitrogen reduction. Applied Catalysis B: Environmental, 2019, 257, 117896.	20.2	220
24	Activation of Ni Particles into Single Ni–N Atoms for Efficient Electrochemical Reduction of CO ₂ . Advanced Energy Materials, 2020, 10, 1903068.	19.5	210
25	Machine learning for renewable energy materials. Journal of Materials Chemistry A, 2019, 7, 17096-17117.	10.3	207
26	Selective nitrogen capture by porous hybrid materials containing accessible transition metal ion sites. Nature Materials, 2017, 16, 526-531.	27.5	201
27	Inverse Design of Solid-State Materials via a Continuous Representation. Matter, 2019, 1, 1370-1384.	10.0	198
28	High capacity carbon dioxide adsorption by inexpensive covalent organic polymers. Journal of Materials Chemistry, 2012, 22, 8431.	6.7	187
29	TiC- and TiN-Supported Single-Atom Catalysts for Dramatic Improvements in CO ₂ Electrochemical Reduction to CH ₄ . ACS Energy Letters, 2017, 2, 969-975.	17.4	186
30	Auxiliary basis expansions for large-scale electronic structure calculations. Proceedings of the National Academy of Sciences of the United States of America, 2005, 102, 6692-6697.	7.1	184
31	Carbon nanofluidics of rapid water transport for energy applications. Chemical Society Reviews, 2014, 43, 565-576.	38.1	179
32	Carbon-supported Ni nanoparticles for efficient CO ₂ electroreduction. Chemical Science, 2018, 9, 8775-8780.	7.4	179
33	Skeletal Octahedral Nanoframe with Cartesian Coordinates <i>via</i> Geometrically Precise Nanoscale Phase Segregation in a Pt@Ni Core–Shell Nanocrystal. ACS Nano, 2015, 9, 2856-2867.	14.6	176
34	Critical Role of Crystal Water for a Layered Cathode Material in Sodium Ion Batteries. Chemistry of Materials, 2015, 27, 3721-3725.	6.7	174
35	Heterogeneous Catalysis for Lithium–Sulfur Batteries: Enhanced Rate Performance by Promoting Polysulfide Fragmentations. ACS Energy Letters, 2017, 2, 327-333.	17.4	174
36	Selective Heterogeneous CO ₂ Electroreduction to Methanol. ACS Catalysis, 2015, 5, 965-971.	11.2	167

#	Article	IF	CITATIONS
37	Anomalous Manganese Activation of a Pyrophosphate Cathode in Sodium Ion Batteries: A Combined Experimental and Theoretical Study. Journal of the American Chemical Society, 2013, 135, 2787-2792.	13.7	165
38	Porous cationic polymers: the impact of counteranions and charges on CO ₂ capture and conversion. Chemical Communications, 2016, 52, 934-937.	4.1	162
39	Exploring the possibilities of two-dimensional transition metal carbides as anode materials for sodium batteries. Physical Chemistry Chemical Physics, 2015, 17, 5000-5005.	2.8	159
40	Rollover Cyclometalation Pathway in Rhodium Catalysis: Dramatic NHC Effects in the C–H Bond Functionalization. Journal of the American Chemical Society, 2012, 134, 17778-17788.	13.7	157
41	On the mechanism of electrochemical ammonia synthesis on the Ru catalyst. Physical Chemistry Chemical Physics, 2016, 18, 9161-9166.	2.8	155
42	Oxygen vacancy enables electrochemical N2 fixation over WO3 with tailored structure. Nano Energy, 2019, 62, 869-875.	16.0	150
43	Hydrogen-Bond-Assisted Controlled C–H Functionalization via Adaptive Recognition of a Purine Directing Group. Journal of the American Chemical Society, 2014, 136, 1132-1140.	13.7	146
44	Stability, Molecular Sieving, and Ion Diffusion Selectivity of a Lamellar Membrane from Two-Dimensional Molybdenum Disulfide. Nano Letters, 2017, 17, 2342-2348.	9.1	144
45	A fast doubly hybrid density functional method close to chemical accuracy using a local opposite spin ansatz. Proceedings of the National Academy of Sciences of the United States of America, 2011, 108, 19896-19900.	7.1	143
46	Role of intermediate phase for stable cycling of Na ₇ V ₄ (P ₂ O) Tj ETQq(Academy of Sciences of the United States of America, 2014, 111, 599-604.	0 0 rgBT 7.1	/Overlock 10 136
47	Highly Stable Nanoporous Sulfurâ€Bridged Covalent Organic Polymers for Carbon Dioxide Removal. Advanced Functional Materials, 2013, 23, 2270-2276.	14.9	135
48	Improved reversibility in lithium-oxygen battery: Understanding elementary reactions and surface charge engineering of metal alloy catalyst. Scientific Reports, 2014, 4, 4225.	3.3	133
49	Directing the Structural Features of N ₂ â€Phobic Nanoporous Covalent Organic Polymers for CO ₂ Capture and Separation. Chemistry - A European Journal, 2014, 20, 772-780.	3.3	128
50	New Insights into the Structure of the Vapor/Water Interface from Large-Scale First-Principles Simulations. Journal of Physical Chemistry Letters, 2011, 2, 105-113.	4.6	126
51	Tuning Metal–Organic Frameworks with Open-Metal Sites and Its Origin for Enhancing CO ₂ Affinity by Metal Substitution. Journal of Physical Chemistry Letters, 2012, 3, 826-829.	4.6	116
52	Highly stable two-dimensional bismuth metal-organic frameworks for efficient electrochemical reduction of CO2. Applied Catalysis B: Environmental, 2020, 277, 119241.	20.2	109
53	How Diradicaloid Is a Stable Diradical?. ChemPhysChem, 2003, 4, 522-525.	2.1	107
54	Highly Efficient Catalytic Cyclic Carbonate Formation by Pyridyl Salicylimines. ACS Applied Materials & Interfaces, 2018, 10, 9478-9484.	8.0	103

#	Article	IF	CITATIONS
55	Generative Adversarial Networks for Crystal Structure Prediction. ACS Central Science, 2020, 6, 1412-1420.	11.3	102
56	The Role of Adsorbed CN and Cl on an Au Electrode for Electrochemical CO ₂ Reduction. ACS Catalysis, 2018, 8, 1178-1185.	11.2	98
57	Stabilization of Cu ⁺ by tuning a CuO–CeO ₂ interface for selective electrochemical CO ₂ reduction to ethylene. Green Chemistry, 2020, 22, 6540-6546.	9.0	98
58	Ab Initio Quantum Chemistry Calculations on the Electronic Structure of Heavier Alkyne Congeners:Â Diradical Character and Reactivity. Journal of the American Chemical Society, 2006, 128, 7185-7192.	13.7	97
59	High-yield production of few-layer boron nanosheets for efficient electrocatalytic N ₂ reduction. Chemical Communications, 2019, 55, 4246-4249.	4.1	96
60	Bifunctional Interface of Au and Cu for Improved CO ₂ Electroreduction. ACS Applied Materials & amp; Interfaces, 2016, 8, 23022-23027.	8.0	93
61	Doping palladium with tellurium for the highly selective electrocatalytic reduction of aqueous CO ₂ to CO. Chemical Science, 2018, 9, 483-487.	7.4	93
62	A Resolution-Of-The-Identity Implementation of the Local Triatomics-In-Molecules Model for Second-Order MÃ,llerâ^Plesset Perturbation Theory with Application to Alanine Tetrapeptide Conformational Energies. Journal of Chemical Theory and Computation, 2005, 1, 862-876.	5.3	90
63	Machine-enabled inverse design of inorganic solid materials: promises and challenges. Chemical Science, 2020, 11, 4871-4881.	7.4	88
64	Aromaticity of Four-Membered-Ring 6π-Electron Systems:  N2S2 and Li2C4H4. Journal of the American Chemical Society, 2004, 126, 3132-3138.	13.7	86
65	Nanostructuring one-dimensional and amorphous lithium peroxide for high round-trip efficiency in lithium-oxygen batteries. Nature Communications, 2018, 9, 680.	12.8	85
66	Mixed Transition Metal Oxide with Vacancy-Induced Lattice Distortion for Enhanced Catalytic Activity of Oxygen Evolution Reaction. ACS Catalysis, 2019, 9, 7099-7108.	11.2	85
67	What is the nature of the long bond in the TCNE22â^ï€-dimer?. Physical Chemistry Chemical Physics, 2004, 6, 2008-2011.	2.8	83
68	Scaled Opposite Spin Second Order MÃ,llerâ^'Plesset Theory with Improved Physical Description of Long-Range Dispersion Interactions. Journal of Physical Chemistry A, 2005, 109, 7598-7605.	2.5	83
69	Active learning with non- <i>ab initio</i> input features toward efficient CO ₂ reduction catalysts. Chemical Science, 2018, 9, 5152-5159.	7.4	82
70	Boosting hot electron flux and catalytic activity at metal–oxide interfaces of PtCo bimetallic nanoparticles. Nature Communications, 2018, 9, 2235.	12.8	80
71	Interaction Mediator Assisted Synthesis of Mesoporous Molybdenum Carbide: Mo-Valence State Adjustment for Optimizing Hydrogen Evolution. ACS Nano, 2020, 14, 4988-4999.	14.6	80
72	Amidoximes: promising candidates for CO2 capture. Energy and Environmental Science, 2011, 4, 4528.	30.8	79

#	Article	IF	CITATIONS
73	Selective electrocatalysis imparted by metal–insulator transition for durability enhancement of automotive fuel cells. Nature Catalysis, 2020, 3, 639-648.	34.4	79
74	Understanding potential-dependent competition between electrocatalytic dinitrogen and proton reduction reactions. Nature Communications, 2021, 12, 4353.	12.8	78
75	Defect ontrolled Formation of Triclinic Na ₂ CoP ₂ O ₇ for 4â€V Sodiumâ€ion Batteries. Angewandte Chemie - International Edition, 2016, 55, 6662-6666.	13.8	76
76	Adsorbate-driven reactive interfacial Pt-NiO _{1â^{~,} <i>x</i>} nanostructure formation on the Pt ₃ Ni(111) alloy surface. Science Advances, 2018, 4, eaat3151.	10.3	76
77	Safeguarding the RuO ₂ phase against lattice oxygen oxidation during acidic water electrooxidation. Energy and Environmental Science, 2022, 15, 1119-1130.	30.8	66
78	Reduced graphene oxides with engineered defects enable efficient electrochemical reduction of dinitrogen to ammonia in wide pH range. Nano Energy, 2020, 68, 104323.	16.0	64
79	A fast correlated electronic structure method for computing interaction energies of large van der Waals complexes applied to the fullerene–porphyrin dimer. Physical Chemistry Chemical Physics, 2006, 8, 2831-2840.	2.8	63
80	Practical Deep-Learning Representation for Fast Heterogeneous Catalyst Screening. Journal of Physical Chemistry Letters, 2020, 11, 3185-3191.	4.6	63
81	Highly durable fuel cell catalysts using crosslinkable block copolymer-based carbon supports with ultralow Pt loadings. Energy and Environmental Science, 2020, 13, 4921-4929.	30.8	61
82	Between Scylla and Charybdis: Hydrophobic Graphene-Guided Water Diffusion on Hydrophilic Substrates. Scientific Reports, 2013, 3, 2309.	3.3	60
83	On the mechanism of high product selectivity for HCOOH using Pb in CO ₂ electroreduction. Physical Chemistry Chemical Physics, 2016, 18, 9652-9657.	2.8	60
84	Fast evaluation of scaled opposite spin second-order MÃ,ller–Plesset correlation energies using auxiliary basis expansions and exploiting sparsity. Journal of Computational Chemistry, 2007, 28, 1953-1964.	3.3	59
85	On the absolute thermodynamics of water from computer simulations: A comparison of first-principles molecular dynamics, reactive and empirical force fields. Journal of Chemical Physics, 2012, 137, 244507.	3.0	59
86	Structure-Based Synthesizability Prediction of Crystals Using Partially Supervised Learning. Journal of the American Chemical Society, 2020, 142, 18836-18843.	13.7	59
87	An invertible crystallographic representation for general inverse design of inorganic crystals with targeted properties. Matter, 2022, 5, 314-335.	10.0	59
88	Controlling the Extent of Diradical Character by Utilizing Neighboring Group Interactions. Journal of Physical Chemistry A, 2003, 107, 7475-7481.	2.5	56
89	Size effect of RhPt bimetallic nanoparticles in catalytic activity of CO oxidation: Role of surface segregation. Catalysis Today, 2012, 181, 133-137.	4.4	54
90	Computational exploration of borophane-supported single transition metal atoms as potential oxygen reduction and evolution electrocatalysts. Physical Chemistry Chemical Physics, 2018, 20, 21095-21104.	2.8	54

#	Article	IF	CITATIONS
91	Ambient Stabilization of Few Layer Phosphorene via Noncovalent Functionalization with Surfactants: Systematic 2D NMR Characterization in Aqueous Dispersion. Chemistry of Materials, 2019, 31, 2786-2794.	6.7	54
92	Highly active and selective Au thin layer on Cu polycrystalline surface prepared by galvanic displacement for the electrochemical reduction of CO2 to CO. Applied Catalysis B: Environmental, 2017, 213, 211-215.	20.2	53
93	Flow-induced voltage generation in non-ionic liquids over monolayer graphene. Applied Physics Letters, 2013, 102, .	3.3	52
94	Phenol-benzene complexation dynamics: Quantum chemistry calculation, molecular dynamics simulations, and two dimensional IR spectroscopy. Journal of Chemical Physics, 2006, 125, 244508.	3.0	49
95	Cycloaddition of Benzene on Si(100) and Its Surface Conversions. Journal of the American Chemical Society, 2005, 127, 3131-3139.	13.7	48
96	The binding nature of light hydrocarbons on Fe/MOF-74 for gas separation. Physical Chemistry Chemical Physics, 2013, 15, 19644.	2.8	46
97	Efficient visible-light driven N ₂ fixation over two-dimensional Sb/TiO ₂ composites. Chemical Communications, 2019, 55, 7171-7174.	4.1	46
98	Progress in Computational and Machineâ€Learning Methods for Heterogeneous Smallâ€Molecule Activation. Advanced Materials, 2020, 32, e1907865.	21.0	46
99	High Facets on Nanowrinkled Cu via Chemical Vapor Deposition Graphene Growth for Efficient CO ₂ Reduction into Ethanol. ACS Catalysis, 2021, 11, 5658-5665.	11.2	46
100	Origin of Selective Guest-Induced Magnetism Transition in Fe/MOF-74. Journal of Physical Chemistry Letters, 2013, 4, 2530-2534.	4.6	45
101	Are both symmetric and buckled dimers on Si(100) minima? Density functional and multireference perturbation theory calculations. Journal of Chemical Physics, 2003, 119, 10917-10923.	3.0	42
102	Observation of the wrapping mechanism in amine carbon dioxide molecular interactions on heterogeneous sorbents. Physical Chemistry Chemical Physics, 2016, 18, 14177-14181.	2.8	42
103	Deep Retrosynthetic Reaction Prediction using Local Reactivity and Global Attention. Jacs Au, 2021, 1, 1612-1620.	7.9	41
104	Diamineâ€Functionalization of a Metal–Organic Framework Adsorbent for Superb Carbon Dioxide Adsorption and Desorption Properties. ChemSusChem, 2018, 11, 1694-1707.	6.8	40
105	Aqueous lithium-ion batteries with niobium tungsten oxide anodes for superior volumetric and rate capability. Energy Storage Materials, 2020, 27, 506-513.	18.0	40
106	Adsorption of Water on the Si(100) Surface:  An Ab Initio and QM/MM Cluster Study. Journal of Physical Chemistry B, 2001, 105, 4039-4044.	2.6	39
107	Accurate Ab Initio-Based Force Field for Predictive CO ₂ Uptake Simulations in MOFs and ZIFs: Development and Applications for MTV-MOFs. Journal of Physical Chemistry C, 2012, 116, 20254-20261.	3.1	39
108	Tungsten Carbide as a Highly Efficient Catalyst for Polysulfide Fragmentations in Li–S Batteries. Journal of Physical Chemistry C, 2018, 122, 7664-7669.	3.1	39

#	Article	IF	CITATIONS
109	Enhanced electrochemical CO2 reduction to ethylene over CuO by synergistically tuning oxygen vacancies and metal doping. Cell Reports Physical Science, 2021, 2, 100356.	5.6	39
110	Site-Specific Transition Metal Occupation in Multicomponent Pyrophosphate for Improved Electrochemical and Thermal Properties in Lithium Battery Cathodes: A Combined Experimental and Theoretical Study. Journal of the American Chemical Society, 2012, 134, 11740-11748.	13.7	37
111	Surface-engineered oxidized two-dimensional Sb for efficient visible light-driven N2 fixation. Nano Energy, 2020, 78, 105368.	16.0	37
112	Understanding the Effects of Au Morphology on CO ₂ Electrocatalysis. Journal of Physical Chemistry C, 2018, 122, 4274-4280.	3.1	36
113	Combinatorial Screening of Highly Active Pd Binary Catalysts for Electrochemical Oxygen Reduction. ACS Combinatorial Science, 2012, 14, 10-16.	3.8	35
114	Multilayer Two-Dimensional Water Structure Confined in MoS ₂ . Journal of Physical Chemistry C, 2017, 121, 16021-16028.	3.1	35
115	Intramolecular Aromatic Carbenoid Insertion of Biaryldiazoacetates for the Regioselective Synthesis of Fluorenes. Chemistry - an Asian Journal, 2011, 6, 2040-2047.	3.3	34
116	Systematic Investigation of the Effect of Polymerization Routes on the Gasâ€Sorption Properties of Nanoporous Azobenzene Polymers. Chemistry - A European Journal, 2015, 21, 15320-15327.	3.3	34
117	Vertical-crystalline Fe-doped Î ² -Ni oxyhydroxides for highly active and stable oxygen evolution reaction. Matter, 2021, 4, 3585-3604.	10.0	34
118	Single atom and defect engineering of CuO for efficient electrochemical reduction of CO ₂ to C ₂ H ₄ . SmartMat, 2022, 3, 194-205.	10.7	34
119	Autobifunctional Mechanism of Jagged Pt Nanowires for Hydrogen Evolution Kinetics via End-to-End Simulation. Journal of the American Chemical Society, 2021, 143, 5355-5363.	13.7	33
120	Studies on Catalytic Activity of Hydrogen Peroxide Generation according to Au Shell Thickness of Pd/Au Nanocubes. ACS Applied Materials & Interfaces, 2018, 10, 38109-38116.	8.0	32
121	Revealing the Role of Oxygen Debris and Functional Groups on the Water Flux and Molecular Separation of Graphene Oxide Membrane: A Combined Experimental and Theoretical Study. Journal of Physical Chemistry C, 2018, 122, 17507-17517.	3.1	32
122	Origin of unusual spinel-to-layered phase transformation by crystal water. Chemical Science, 2018, 9, 433-438.	7.4	31
123	Single yttrium sites on carbon-coated TiO ₂ for efficient electrocatalytic N ₂ reduction. Chemical Communications, 2020, 56, 10910-10913.	4.1	31
124	Uncertainty-Quantified Hybrid Machine Learning/Density Functional Theory High Throughput Screening Method for Crystals. Journal of Chemical Information and Modeling, 2020, 60, 1996-2003.	5.4	31
125	Adsorption of Carbon Dioxide on Unsaturated Metal Sites in M ₂ (dobpdc) Frameworks with Exceptional Structural Stability and Relation between Lewis Acidity and Adsorption Enthalpy. Chemistry - A European Journal, 2016, 22, 7444-7451.	3.3	30
126	Can Metal–Organic Framework Separate 1-Butene from Butene Isomers?. Journal of Physical Chemistry Letters, 2014, 5, 440-446.	4.6	29

#	Article	IF	CITATIONS
127	Importance of Ligand Effects Breaking the Scaling Relation for Core–Shell Oxygen Reduction Catalysts. ChemCatChem, 2017, 9, 3173-3179.	3.7	28
128	Effects of boron oxidation state on electrocatalytic activity of carbons synthesized from CO ₂ . Journal of Materials Chemistry A, 2015, 3, 5843-5849.	10.3	27
129	Ti(N ₅) ₄ as a Potential Nitrogen-Rich Stable High-Energy Density Material. Journal of Physical Chemistry A, 2016, 120, 4249-4255.	2.5	27
130	One dimensional building blocks for molecular separation: laminated graphitic nanoribbons. Nanoscale, 2017, 9, 19114-19123.	5.6	27
131	Activating Transition Metal Dichalcogenides by Substitutional Nitrogenâ€Đoping for Potential ORR Electrocatalysts. ChemElectroChem, 2018, 5, 4029-4035.	3.4	27
132	Towards stable Na-rich layered transition metal oxides for high energy density sodium-ion batteries. Energy Storage Materials, 2020, 25, 62-69.	18.0	27
133	Probing surface oxide formations on SiO ₂ -supported platinum nanocatalysts under CO oxidation. RSC Advances, 2017, 7, 45003-45009.	3.6	26
134	Ordered Supramolecular Gels Based on Graphene Oxide and Tetracationic Cyclophanes. Advanced Materials, 2014, 26, 2725-2729.	21.0	25
135	Mechanistic Study on C–C Bond Formation of a Nickel(I) Monocarbonyl Species with Alkyl Iodides: Experimental and Computational Investigations. Organometallics, 2015, 34, 4305-4311.	2.3	25
136	Direct observation of atomic hydrogen generated from the water framework of clathrate hydrates. Chemical Communications, 2011, 47, 674-676.	4.1	24
137	Tuning the Pd-catalyzed electroreduction of CO ₂ to CO with reduced overpotential. Catalysis Science and Technology, 2018, 8, 3894-3900.	4.1	24
138	Modulating the magnetic behavior of Fe(<scp>ii</scp>)–MOF-74 by the high electron affinity of the guest molecule. Physical Chemistry Chemical Physics, 2015, 17, 16977-16982.	2.8	23
139	Analytical Double-Hybrid Density Functional Based on the Polynomial Series Expansion of Adiabatic Connection: A Quadratic Approximation. Journal of Chemical Theory and Computation, 2015, 11, 45-54.	5.3	22
140	Ultralow Overpotential of Hydrogen Evolution Reaction using Feâ€Doped Defective Graphene: A Density Functional Study. ChemCatChem, 2018, 10, 4450-4455.	3.7	22
141	Flow-induced voltage generation over monolayer graphene in the presence of herringbone grooves. Nanoscale Research Letters, 2013, 8, 487.	5.7	21
142	A Novel Fabrication of 3.6 nm High Graphene Nanochannels for Ultrafast Ion Transport. Advanced Materials, 2017, 29, 1605854.	21.0	21
143	Lattice Convolutional Neural Network Modeling of Adsorbate Coverage Effects. Journal of Physical Chemistry C, 2019, 123, 18951-18959.	3.1	21
144	Enhanced rate capability due to highly active Ta2O5 catalysts for lithium sulfur batteries. Journal of Power Sources, 2019, 435, 226707.	7.8	21

#	Article	IF	CITATIONS
145	Protruding interfacial OH groups and â€~on-water' heterogeneous catalysis. Journal of Physics Condensed Matter, 2010, 22, 284117.	1.8	20
146	pH-Dependent Conformations for Hyperbranched Poly(ethylenimine) from All-Atom Molecular Dynamics. Macromolecules, 2018, 51, 2187-2194.	4.8	20
147	Controlling hot electron flux and catalytic selectivity with nanoscale metal-oxide interfaces. Nature Communications, 2021, 12, 40.	12.8	20
148	Polyselenide Anchoring Using Transition-Metal Disulfides for Enhanced Lithium–Selenium Batteries. Inorganic Chemistry, 2018, 57, 2149-2156.	4.0	19
149	An ab initio study of the structure of two-, three- and five-dimersilicon clusters: An approach to the Si(100) surface. Theoretical Chemistry Accounts, 2003, 109, 268-273.	1.4	18
150	A Fast Implementation of Perfect Pairing and Imperfect Pairing Using the Resolution of the Identity Approximation. Journal of Chemical Theory and Computation, 2006, 2, 300-305.	5.3	18
151	Comment on "Inaccuracy of Density Functional Theory Calculations for Dihydrogen Binding Energetics onto Ca Cation Centers― Physical Review Letters, 2010, 104, 179601; author reply 179602.	7.8	18
152	Alcohol Dimer is Requisite to Form an Alkyl Oxonium Ion in the Proton Transfer of a Strong (Photo)Acid to Alcohol. Chemistry - A European Journal, 2016, 22, 4340-4344.	3.3	18
153	A catalytic role of surface silanol groups in CO ₂ capture on the amine-anchored silica support. Physical Chemistry Chemical Physics, 2018, 20, 12149-12156.	2.8	18
154	Unveiling new stable manganese based photoanode materials <i>via</i> theoretical high-throughput screening and experiments. Chemical Communications, 2019, 55, 13418-13421.	4.1	18
155	Longitudinal unzipping of 2D transition metal dichalcogenides. Nature Communications, 2020, 11, 5032.	12.8	18
156	Superexchange-Like Interaction of Encaged Molecular Oxygen in Nitrogen-Doped Water Cages of Clathrate Hydrates. Journal of the American Chemical Society, 2011, 133, 20399-20404.	13.7	17
157	Predictions of the sulfur and carbon kinetic isotope effects in the OH + OCS reaction. Chemical Physics Letters, 2012, 531, 64-69.	2.6	17
158	Engineering vacancy and hydrophobicity of two-dimensional TaTe2 for efficient and stable electrocatalytic N2 reduction. Innovation(China), 2022, 3, 100190.	9.1	16
159	Perovskite synthesizability using graph neural networks. Npj Computational Materials, 2022, 8, .	8.7	16
160	Analytic Derivatives of Quartic-Scaling Doubly Hybrid XYGJ-OS Functional: Theory, Implementation, and Benchmark Comparison with M06-2X and MP2 Geometries for Nonbonded Complexes. Journal of Chemical Theory and Computation, 2013, 9, 1971-1976.	5.3	15
161	Computational Analysis of Pressure-Dependent Optimal Pore Size for CO ₂ Capture with Graphitic Surfaces. Journal of Physical Chemistry C, 2016, 120, 3978-3985.	3.1	15
162	Intrinsic Relation between Hot Electron Flux and Catalytic Selectivity during Methanol Oxidation. ACS Catalysis, 2019, 9, 8424-8432.	11.2	15

#	Article	IF	CITATIONS
163	Microscopic structure and dynamics of air/water interface by computer simulations—comparison with sum-frequency generation experiments. Physical Chemistry Chemical Physics, 2011, 13, 5388.	2.8	14
164	A potential role of a substrate as a base for the deprotonation pathway in Rh-catalysed C–H amination of heteroarenes: DFT insights. Dalton Transactions, 2016, 45, 7980-7985.	3.3	14
165	Tuning the Phase Stability of Sodium Metal Pyrophosphates for Synthesis of High Voltage Cathode Materials. Chemistry of Materials, 2016, 28, 6724-6730.	6.7	14
166	Shifting the scaling relations of single-atom catalysts for facile methane activation by tuning the coordination number. Chemical Science, 2021, 12, 3551-3557.	7.4	14
167	Tunable sieving of small gas molecules using horizontal graphene oxide membrane. Journal of Membrane Science, 2020, 610, 118178.	8.2	14
168	Bimetallic Gold–Silver Nanostructures Drive Low Overpotentials for Electrochemical Carbon Dioxide Reduction. ACS Applied Materials & Interfaces, 2022, 14, 6604-6614.	8.0	14
169	An Orbital-Based Definition of Radical and Multiradical Character. Journal of Physical Chemistry A, 2004, 108, 10270-10279.	2.5	13
170	The critical size of hydrogen-bonded alcohol clusters as effective BrÃ,nsted bases in solutions. Physical Chemistry Chemical Physics, 2016, 18, 24880-24889.	2.8	13
171	Edge-Functionalized Graphene Nanoribbon Frameworks for the Capture and Separation of Greenhouse Gases. Macromolecules, 2017, 50, 523-533.	4.8	13
172	A local environment descriptor for machine-learned density functional theory at the generalized gradient approximation level. Journal of Chemical Physics, 2018, 148, 241742.	3.0	13
173	Assessments of Semilocal Density Functionals and Corrections for Carbon Dioxide Adsorption on Metal–Organic Frameworks. ChemPhysChem, 2014, 15, 3157-3165.	2.1	11
174	Optimal Activation of Porous Carbon for High Performance CO ₂ Capture. ChemNanoMat, 2016, 2, 528-533.	2.8	11
175	Low-Dimensional Confined Ice Has the Electronic Signature of Liquid Water. Journal of Physical Chemistry Letters, 2019, 10, 2008-2016.	4.6	11
176	Artificial neural network for the configuration problem in solids. Journal of Chemical Physics, 2017, 146, 064103.	3.0	10
177	Alteration of oxygen evolution mechanisms in layered LiCoO ₂ structures by intercalation of alkali metal ions. Journal of Materials Chemistry A, 2022, 10, 10967-10978.	10.3	10
178	Charge-transfer descriptor for the cycle performance of β-Li ₂ MO ₃ cathodes: role of oxygen dimers. Journal of Materials Chemistry A, 2020, 8, 2663-2671.	10.3	9
179	Stability of Positively Charged Solutes in Water: A Transition from Hydrophobic to Hydrophilic. Journal of Physical Chemistry Letters, 2012, 3, 294-298.	4.6	8
180	Local intermolecular interactions for selective CO2 capture by zeolitic imidazole frameworks: energy decomposition analysis. Journal of Nanoparticle Research, 2012, 14, 1.	1.9	8

#	Article	IF	CITATIONS
181	Pd ₃ Pb Nanosponges for Selective Conversion of Furfural to Furfuryl Alcohol under Mild Condition. Small Methods, 2021, 5, e2100400.	8.6	8
182	Automated exploitation of the big configuration space of large adsorbates on transition metals reveals chemistry feasibility. Nature Communications, 2022, 13, 2087.	12.8	8
183	A perspective on the density matrix purification for linear scaling electronic structure calculations. International Journal of Quantum Chemistry, 2016, 116, 563-568.	2.0	7
184	Theoretical Study on the Degree of CO ₂ Activation in CO ₂ -Coordinated Ni(0) Complexes. ACS Omega, 2021, 6, 7646-7654.	3.5	7
185	Accelerated Purification Using Generalized Nonpurifying Intermediate Functions for Large-Scale Self-Consistent Field Calculations. Journal of Chemical Theory and Computation, 2011, 7, 3853-3858.	5.3	6
186	On the structure of Si(100) surface: Importance of higher order correlations for buckled dimer. Journal of Chemical Physics, 2013, 138, 204709.	3.0	6
187	On the optimal symmetric purification scheme of the one-particle density matrix. Chemical Physics Letters, 2011, 511, 159-160.	2.6	5
188	A perspective on the electronic structure calculations for properties of battery electrode materials. International Journal of Quantum Chemistry, 2015, 115, 1141-1146.	2.0	5
189	Defectâ€Controlled Formation of Triclinic Na ₂ CoP ₂ O ₇ for 4â€V Sodiumâ€lon Batteries. Angewandte Chemie, 2016, 128, 6774-6778.	2.0	5
190	Unexpected solution phase formation of hollow PtSn alloy nanoparticles from Sn deposition on Pt dendritic structures. CrystEngComm, 2016, 18, 6019-6023.	2.6	5
191	Classifying Intermetallic Tetragonal Phase of All-d-Metal Heusler Alloys for Catalysis Applications. Topics in Catalysis, 2022, 65, 208-214.	2.8	5
192	Correction and Addition to "Tuning Metal–Organic Frameworks with Open-Metal Sites and Its Origin for Enhancing CO ₂ Affinity by Metal Substitution― Journal of Physical Chemistry Letters, 2012, 3, 1582-1582.	4.6	4
193	A soft damping function for dispersion corrections with less overfitting. Journal of Chemical Physics, 2016, 145, 174104.	3.0	4
194	Surface overgrowth on gold nanoparticles modulating high-energy facets for efficient electrochemical CO2 reduction. Nanoscale, 2021, 13, 14346-14353.	5.6	4
195	Heterogeneous Catalysis in Grammar School. Journal of Physical Chemistry C, 2022, 126, 2931-2936.	3.1	4
196	Recent progress in computational discovery of Heusler alloys. Bulletin of the Korean Chemical Society, 2022, 43, 484-491.	1.9	4
197	Correlated Local Fluctuations in the Hydrogen Bond Network of Liquid Water. Journal of the American Chemical Society, 2022, 144, 13127-13136.	13.7	4
198	Fast electronic structure methods for strongly correlated molecular systems. Journal of Physics: Conference Series, 2005, 16, 233-242.	0.4	3

#	Article	IF	CITATIONS
199	Predicting potentially hazardous chemical reactions using an explainable neural network. Chemical Science, 2021, 12, 11028-11037.	7.4	3
200	Molecular dynamics simulations for thermal transport behavior of InAs nanotubes: A role of symmetry. Computational Materials Science, 2013, 70, 8-12.	3.0	2
201	Infrared spectroscopy and density functional calculations on titanium-dinitrogen complexes. Chemical Physics Letters, 2018, 698, 163-170.	2.6	2
202	Effects of ligands and spin-polarization on the preferred conformation of distannynes. Dalton Transactions, 2008, , 4428.	3.3	1
203	Alcohol Dimer is Requisite to Form an Alkyl Oxonium Ion in the Proton Transfer of a Strong (Photo)Acid to Alcohol. Chemistry - A European Journal, 2016, 22, 4301-4301.	3.3	1
204	Reply to Comment on â€~On the optimal symmetric purification scheme of the one-particle density matrix'. Chemical Physics Letters, 2012, 527, 86-88.	2.6	0
205	Theoretical chemistry in Korea: Professor Yoon Sup Lee and the early stages of theoretical chemistry in Korea. International Journal of Quantum Chemistry, 2016, 116, 561-562.	2.0	0
206	EEWS 2016: Progress and Perspectives of Energy Science and Technology. ACS Energy Letters, 2017, 2, 592-594.	17.4	0
207	Local intermolecular interactions for selective CO2 capture by zeolitic imidazole frameworks: energy decomposition analysis. , 2012, , 277-288.		0